Asian Journal of Chemistry; Vol. 38, No. 6 (2026), 1471-1481
ASIAN JOURNAL OF CHEMISTRY
https://doi.org/10.14233/ajchem.2026.35715

Synthesis of Medicinally Relevant Pro-Pro Dipeptide as Antidiabetic, Anti-inflammatory and Antioxidant: Molecular Docking and Drug-Likeness

SOLOMON IZUCHI ATTAH[1,*], UCHECHUKWU CHRIS OKORO[1], IFEOMA VIVIAN OKONKWO[2], FIDELIA NGOZI IBEANU[3], PRECIOUS KELECHI ATTAH[1] and COSMAS CHINWEIKE EZE[3]

[1]Department of Pure and Industrial Chemistry, University of Nigeria, Nsuuka, Nigeria
[2]Department of Science Laboratory Technology, Faculty of Physical Sciences, University of Nigeria, Nsuuka, Nigeria
[3]Department of Natural Science Unit, School of General Studies, University of Nigeria, Nsuuka, Nigeria

*Corresponding author: E-mail: solomon.attah@unn.edu.ng

Received: 6 February 2026 *Accepted*: 22 April 2026 *Published online*: 31 May 2026 AJC-22373

The choice of design and synthesis of new dipeptide derivatives is due to their broad pharmacological activities against various diseases. In present study, eight novel dipeptides incorporating sulphonamide functionality (**8a-h**) were synthesised *via* the reaction of benzenesulphonyl chloride and L-proline to afford benzenesulphonamides. The condensation reaction of benzenesulphonamides and carboxamide derivatives, using peptide coupling reagents afforded the dipeptide compounds (**8a-h**). The structural validation of the compounds was done using IR, ^{1}H NMR, ^{13}C NMR and MS spectrometry. Molecular docking studies revealed favourable interactions between the compounds and key amino acid residues in the active site of the protein targets. The drug-likeness study showed that the compounds comply with Lipinski's rule of five, indicating strong potential as orally bioavailable candidates. Compound **8a** exhibited superior antidiabetic activity compared to the standard clinical drug, acarbose. Antioxidant screening demonstrated that compound **8g**, with an IC_{50} value of 0.214 µg/mL, exhibited comparable activity to ascorbic acid (IC_{50}: 0.213 µg/mL). In the carrageenan-induced rat paw edema bioassay, at 0.5 h, compounds **8a-h** showed strong anti-inflammatory inhibition with percentage inhibition in the range of 97.67-86.64 %, compared to the reference drug, indomethacin (75.55 %). Some of the dipeptide derivatives are identified as promising therapeutic agents for further studies.

Keywords: Dipeptides, Benzenesulphonamides, L-proline, Biological activities, Pharmacokinetics, Toxicity properties.

INTRODUCTION

Sulphonamides and their analogues to date still retain their pharmacological role as potential candidates in the treatment of diverse illnesses [1-6] and their scaffold remains a delicate area of research for synthetic/medicinal organic chemists [7]. Several reports have confirmed sulphonamides as potential antitubercular [8], anticancer [9], antimicrobial [10] and anti-malarial [11] agents.

Dipeptides and their analogues have shown potential medicinal values and play crucial parts in living organisms [12]. This class of therapeutic agents has been reported as a good antitumor agent, antimicrobial inhibitors and a good reinforcer of peripheral blood lymphocytes in humans [13-15]. Mostly dipeptides bind strongly to membrane receptors; hence, they possess good druggability properties such as solubility, permeability and good oral bioavailability [16]. In recent reports, val-val dipeptides and ala-gly dipeptides have shown interesting biological efficacy as good antioxidants and antimalarial agents [17,18] and this perhaps motivated us to develop pro-pro dipeptides as potential drug candidates targeting inflammatory disease, diabetes disease and other diseases related to oxidative reaction. Several sulphonamides with dipeptide moieties have been reported as good therapeutic agents having good anti-diabetic properties, oxidative stress and anti-inflammatory activity [5,19]. The pharmacological significance of sulphonamides, carboxamides and dipeptides as documented in the literature motivated the authors of this study to continue designing and creating more potent hybrid novel compounds that combine the three molecular backbones of sulphonamides, carboxamides and dipeptides into a single molecular entity.

Studies establish that oxidative stress modulates the actions of inflammatory mediators and inflammation in turn promotes the development of reactive oxygen species [19-21].

Oxidative stress has an important role in the development of diabetes complications [22]. Several illnesses, such as osteoarthritis, infections, psoriasis as well as inflammatory bowel disease, are caused by inflammation [23]. Non-steroidal anti-inflammatory drugs (NSAIDs) are good therapeutic agents available in clinics worldwide for the treatment of inflammation. Presently, NSAIDs therapy has displayed a lot of side effects, ranging from renal dysfunction, gastrointestinal mucosal damage, bleeding and hepatoxicity [24].

To overcome limitations such as drug resistance and the adverse side effects commonly associated with existing drug molecules, the present study focuses on the development of dipeptide-based drug candidates with potent inhibitory activity against the COX-2 enzyme. Over the years, serious concerns have been raised about the global health threat emanating from diabetes. Perhaps, it remains a severe disease affecting humans globally and its root has contributed to the high mortality rate and disability globally [25]. However, clinical drugs such as miglitol, acarbose and voglibose, which are α-glucosidase enzyme inhibitors, act through several mechanisms, *viz*. delay carbohydrate digestion, reduce intestinal adsorption of glucose, boost insulin activity and reduce postprandial rise in blood glucose [26,27]. This class of drugs still displays unfavourable side effects towards humans despite their therapeutic relevance. So far, traceable side effects associated with this drug utilisation include liver damage, kidney dysfunction as well as gastrointestinal problems like stomach ache, diarrhoea and flatulence [28]. Considering all these challenges as reviewed herein, aroused our inspiration as medicinal and synthetic organic chemists to design and go into a deep search for new potent COX-2 enzyme inhibitors. As an extension of our ongoing investigations into the biological properties of sulphonamide-containing dipeptides [29-34], the present study reports the synthesis of novel pro–pro dipeptides incorporating sulphonamide moieties.

EXPERIMENTAL

^{1}H and ^{13}C NMR were obtained from a Bruker AV 400 MHZ for ^{1}H and 101 MHZ for ^{13}C using trimethylsilane as internal standard. Unless otherwise specified, all solvents and chemicals were reagent grade and used as received from Sigma-Aldrich, USA. The mass spectra were obtained using an Agilent Technologies 6510, Q-TOFLC/MS ESI-Technique. Melting points were measured with digital melting point equipment and are uncorrected. The synthesis of the dipeptides were carried out at Indian Institute of Technology Kanpur, India. Thin layer chromatography (TLC) on precoated silica gel was used to track every reaction. For chromatographic separation, Merck neutral aluminum oxide activated (60-325 mesh) was employed.

2-(Phenylsulfonyl)cyclopentane-1-carboxylic acid (2): Following a general procedure [31] to a 250 mL dry two necked fitted flask containing a magnetic stirrer, was charged *L*-proline (2.0 g, 17.37 mmol), diethyl ether (70 mL) and NaOH (12.0 mL, 1.5 M). After stirring for a few minutes, benzenesulfonyl chloride (0.95 g, 6.0 mmol) was added in one portion and the reaction mixture was stirred at room temperature for 20 h. The reaction mixture was washed with diethyl ether and the aqueous layer was acidified to a pH of 3 with a 1 N HCl solution. The aqueous layer was extracted with ethyl acetate (3 × 100 mL). The combined organic extract was dried over anhydrous sodium sulphate and concentrated. The crude was recrystallised in dichloromethane/hexane to give the titled compound in quantitative yield.

General procedure for Boc protection: To a solution of *L*-proline (2.0 g, 26.3 mmol) in 1,4-dioxane/water (60 mL, 2:1 v/v) was added NaOH (1.1 g, 26.3 mmol) at 0 ºC. To this solution was added di-*tert*-butyl dicarbonate (1.1 g, 26.6 mmol) in portions. The reaction mixture was stirred for 1 h and warmed to room temperature. After stirring for an additional 30 min, the reaction mixture was diluted with water and washed with diethyl ether. The aqueous layer was acidified with conc. HCl to pH 1-2 and was extracted with ethyl acetate (3 × 100 mL). The combined organic extract was dried over anhydrous $MgSO_4$ and concentrated to give (*tert*-butoxycarbonyl)-*L*-proline as a white solid which was used without further purification (yield: 4.37 g, 94%).

General procedure for the synthesis of *tert*-butyl-2-(substituted-carbamoyl)pyrrolidine-1-carboxylate (6a-h): A solution of (*tert*-butoxycarbonyl)-*L*-proline (3.0 g, 13.94 mmol, 1.0 equiv.) in anhydrous THF (50 mL) was sequentially treated with triethyl amine (3 equiv.), 1,3-dicyclohexylcarbodiimide (1.1 equiv.), 1*H*-1,2,3-benzotriazol-1-ol (1.1 equiv.), substituted amines **5a-h** (1.0 equiv.). After stirring for 20 h, the reaction mixture was diluted with ethyl acetate and filtered to remove the urea byproduct. The filtrate was washed with water and brine, dried over anhydrous $MgSO_4$ and concentrated. Purification of the crude by column chromatography [aluminum oxide, hexane: ethyl acetate: methanol (5:2:1)] produced the compounds in good yields.

General procedure for the synthesis of (substituted)-pyrrolidine-2-carboxamide (7a-h): A solution of Boc-protected amines **6a-h** (9 mmol) in dry CH_2Cl_2 (40 mL) was treated with trifluoroacetic acid (30 mL) at 0 ºC. After the completion of reaction as indicated by TLC, the reaction mixture was concentrated under reduced pressure. The residue was dissolved in CH_2Cl_2 and basified with 2 N NaOH to a pH of 12. The reaction mixture was extracted with ethyl acetate (3 × 100 mL), dried over anhydrous Na_2SO_4 and concentrated under reduced pressure to give the substituted carboxamides in quantitative yield.

General procedure for the synthesis of *N*-(cyclohexa-1,5-dien-1-yl)-1-((phenyl substituted sulfonyl)-*L*-prolyl)-pyrrolidine-2-carboxamide (8a-h): A solution of 2-(phenylsulfonyl)cyclopentane-1-carboxylic acid (**3**, 0.85 g, 3.3 mmol) in anhydrous THF (20 mL) was treated with triethyl amine (3 equiv.), 1,3-dicyclohexylcarbodiimide (1.1 equiv.), 1*H*-1,2,3-benzotriazol-1-ol (1.1 equiv.), substituted amines **7a-h** (1.0 equiv.). After stirring for 20 h, the reaction mixture was diluted with ethyl acetate and filtered to remove the urea byproduct. The filtrate was washed with water and brine, dried over anhydrous $MgSO_4$ and concentrated (**Scheme-I**). Purification of the crude by column chromatography [AlO_3, hexane: ethyl acetate: methanol (5:2:1)] produced the pro-pro dipeptides.

***N*-(4-Methoxyphenyl)-1-((phenylsulfonyl)prolyl)pyrrolidine-2-carboxamide (8a):** White solid, yield: 0.70 g, 99%); m.p.: 163-165 ºC; ^{1}H NMR (400 MHz, chloroform-d_6, δ ppm):

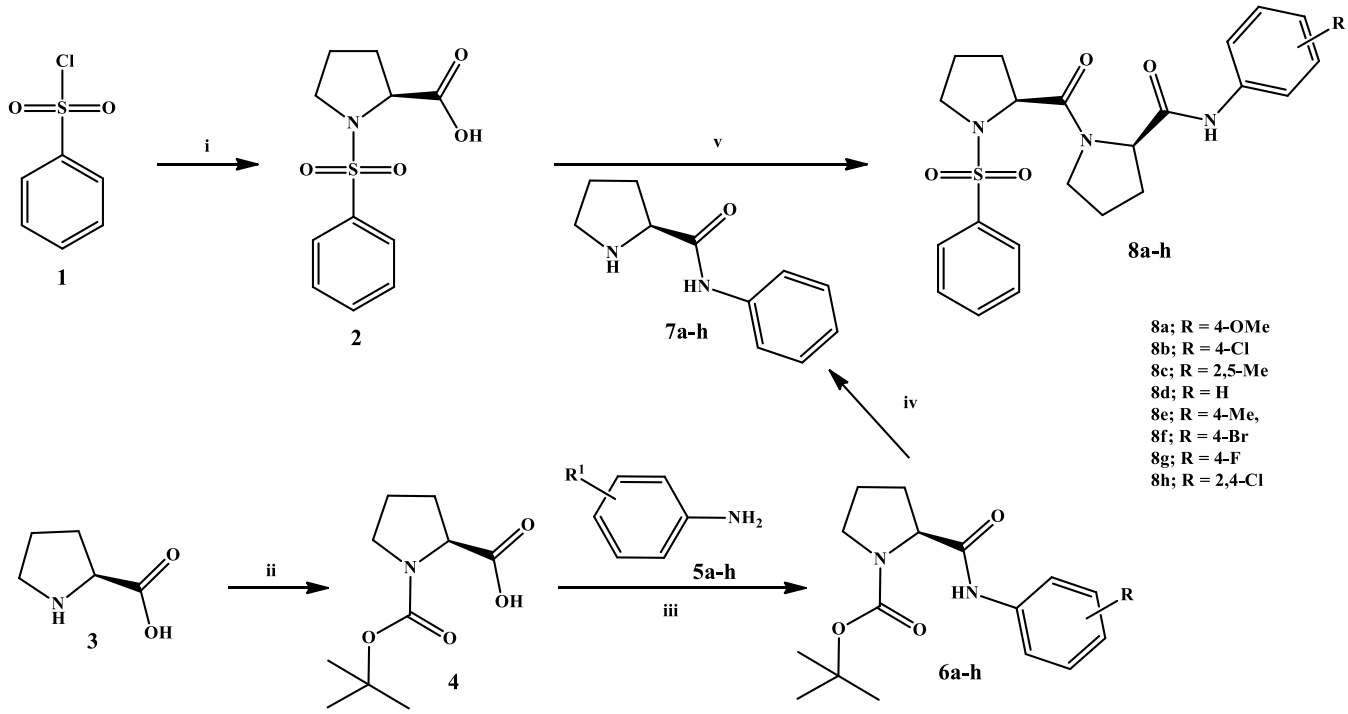

Scheme-I: Synthetic route to Pro-Pro dipeptide-sulphonamides **8a-h**; Conditions: (i) NaOH, diethyl ether, rt, overnight, quant. (ii) di-*tert*-butyl decarbonate, NaOH, dioxane/water, 0 ºC - rt, 1 h, 94% (iii) EDC·HCl, HOBt, THF, triethylamine, 0 ºC-rt, 20 h (iv) TFA, CH_2Cl_2, rt, 1 h quant. (v) EDC·HCl, HOBt, THF, triethylamine, 0 ºC-rt, 20 h, 56%-quant

8.81 (s, 1H, NH), 8.21 (d, *J* = 9.1 Hz, 1H), 7.70 (d, *J* = 8.2 Hz, 2H), 7.18 (d, *J* = 8.1 Hz, 2H), 6.89 (t, *J* = 7.6 Hz, 1H), 6.82 (d, *J* = 8.0 Hz, 1H), 5.86 (s, 1H), 4.61 (d, *J* = 8.2 Hz, 1H), 3.82-3.70 (m, 5H), 3.43 (s, 2H), 3.38-3.29 (m, 1H), 2.31 (s, 4H), 1.98-1.92 (m, 1H), 1.23 (s, 1H), 0.86 (s, 1H). ^{13}C NMR (400 MHz, chloroform-d_6, δ ppm): 168.64 (C=O), 166.93 (C=O), 148.31, 143.80, 135.96, 129.81, 127.51, 127.20, 124.13, 120.92, 119.94, 110.18 (ten aromatic carbons), 61.23, 55.86, 46.43, 44.54, 27.91, 24.80, 21.54 (seven aliphatic carbons); ESI-HRMS (*m/z*): found 457.1882 (M+H), calcd. 457.1883.

***N*-(2,5-Dimethylphenyl)-1-(tosylprolyl)pyrrolidine-2-carboxamide (8b):** White solid, yield: 0.50 g, 88%, m.p.: 188-189 ºC, FTIR (KBr, ν_{max}, cm^{-1}): 3314, 3276 (NH), 3193, 3115, 3062 (C-H arom.), 2930, 2854 (C-H aliph.), 1696, 1643 (2×C=O), 1591, 1537, 1490, 1447 (C=C arom.), 1393, 1348 (2×S=O), 1290, 1248, 1160, 1117 (S-N), 1096, 1072, 1022, 1007 (C-N); ^{1}H NMR (400 MHz, chloroform-d_6, δ ppm): 9.21 (s, 1H, NH), 7.91-7.81 (m, 2H), 7.61-7.48 (m, 1H), 7.01 (d, *J* = 7.6 Hz, 2H), 6.81 (d, *J* = 7.3 Hz, 2H), 4.80 (d, *J* = 7.7 Hz, 2H), 3.55 (t, *J* = 9.1 Hz, 1H), 3.49-3.34 (m, 2H), 2.28 (s, 3H), 2.21 (s, 3H), 2.17 (s, 2H), 2.12 (s, 3H), 1.81 (d, *J* = 7.4 Hz, 4H); ^{13}C NMR (400 MHz, chloroform-d_6, δ ppm): 171.89 (C=O), 169.35 (C=O), 136.68, 136.53, 133.34, 130.55, 129.51, 127.84, 125.86, 125.42, 123.49, 122.59 (ten aromatic carbons), 61.33, 60.62, 59.76, 48.79, 31.06, 27.02, 26.03, 25.53, 22.78, 21.59, 18.02 (eleven aliphatic carbons); ESI-HRMS (*m/z*): found 469.1317 (M+H), calcd. 469.1318.

***N*-(4-Bromophenyl)-1-((phenylsulfonyl)prolyl)pyrrolidine-2-carboxamide (8c):** White solid, yield: 0.56 g, 59%, m.p.: 161-162 ºC, FTIR (KBr, ν_{max}, cm^{-1}): 3314, 3276 (NH), 3193, 3115, 3062 (C-H arom.), 2930, 2854 (C-H aliph.), 1696, 1643 (2C=O), 1591, 1537, 1490, 1447 (C=C arom.), 1393, 1348 (2S=O), 1290, 1248, 1160, 1117 (S-N), 1096, 1072, 1022, 1007 (C-N); ^{1}H NMR (400 MHz, chloroform-d_6, δ ppm): 9.52 (s, 1H), 7.90-7.83 (m, 2H), 7.55 (dt, *J* = 33.1, 7.4 Hz, 3H), 7.39 (d, *J* = 8.8 Hz, 2H), 7.25 (d, *J* = 4.5 Hz, 2H), 4.69 (dd, *J* = 7.1, 3.5 Hz, 1H), 4.46-4.39 (m, 1H), 3.75 (t, *J* = 6.4 Hz, 2H), 3.55-3.44 (m, 1H), 3.37-3.26 (m, 1H), 2.25 (dd, *J* = 9.4, 5.6 Hz, 1H), 2.07 (dtt, *J* = 24.3, 12.6, 6.4 Hz, 5H), 2.00-1.94 (m, 1H), 1.83 (s, 1H). ^{13}C NMR (400 MHz, chloroform-d_6, δ ppm): 171.33 (C=O), 169.61 (C=O), 137.53, 137.34, 132.88, 131.30, 129.03, 127.19, 121.02, 116.01 (eight aromatic carbons), 61.47, 60.23, 48.46, 47.41, 30.19, 27.75, 25.17, 24.59 (eight aliphatic carbons); ESI-HRMS (*m/z*): found 505.0785 (M+H), calcd. 505.0787.

***N*-(2,5-Dimethylphenyl)-1-((phenylsulfonyl)prolyl)pyrrolidine-2-carboxamide (8d):** Black solid, yield: 0.50 g, 58%, m.p.: 117-118 ºC, FTIR (KBr, ν_{max}, cm^{-1}): 3314, 3276 (NH), 3193, 3115, 3062 (C-H arom.), 2930, 2854 (C-H aliph.), 1696, 1643 (2C=O), 1591, 1537, 1490, 1447 (C=C arom.), 1393, 1348 (2S=O), 1290, 1248, 1160, 1117 (S-N), 1096, 1072, 1022, 1007 (C-N); ^{1}H NMR (400 MHz, chloroform-d_6, δ ppm): 9.21 (s, 1H), 7.91-7.81 (m, 2H), 7.61-7.48 (m, 1H), 7.01 (d, *J* = 7.6 Hz, 2H), 6.81 (d, *J* = 7.3 Hz, 2H), 4.80 (d, *J* = 7.7 Hz, 2H), 3.55 (t, *J* = 9.1 Hz, 1H), 3.49-3.34 (m, 2H), 2.28 (s, 3H), 2.21 (s, 3H), 2.17 (s, 2H), 2.12 (s, 3H), 1.81 (d, *J* = 7.4 Hz, 4H); ^{13}C NMR (400 MHz, chloroform-d_6, δ ppm): 171.89 (C=O), 169.35 (C=O), 136.68, 136.53, 133.34, 130.55, 129.51, 127.84, 125.86, 125.42, 123.49, 122.59 (ten aromatic carbons), 61.33, 60.62, 59.76, 48.79, 31.06, 27.02, 25.53, 22.78, 21.59, 18.02 (ten aliphatic carbons); ESI-HRMS (*m/z*): found 455.2870 (M+H), calcd. 455.2870.

***N*-(2-Methoxyphenyl)-1-((phenylsulfonyl)prolyl)pyrrolidine-2-carboxamide (8e):** White solid, yield: 1.00 g, 78%, m.p.: 180-181 ºC, FTIR (KBr, ν_{max}, cm^{-1}): 3407 (NH), 3061 (C-H arom.), 2952, 2878 (C-H aliph.), 1685, 1657 (2×C=O), 1528, 1485, 1436, 1460 (C=C arom.), 1344, 1389 (2×S=O), 1159, 1115 (S-N), 1096, 1072, 1047 (C-N, C-O); ^{1}H NMR (400 MHz, chloroform-d_6, δ ppm): 8.81 (s, 1H, NH), 8.27 (d, *J* = 9.1 Hz, 1H), 7.89 (d, *J* = 7.4 Hz, 2H), 7.59-7.46 (m, 3H), 6.98 (d, *J* = 9.0 Hz, 1H), 6.89 (t, *J* = 7.5 Hz, 1H), 6.82 (d, *J* = 7.5 Hz, 1H), 4.75-4.61 (m, 2H), 3.81 (s, 3H), 3.62 (t, *J* = 7.0 Hz, 1H), 3.49-3.35 (m, 2H), 2.44-2.35 (m, 1H), 2.22-1.94 (m, 8H); ^{13}C NMR (400 MHz, chloroform-d_6, δ ppm): 171.80 (C=O), 169.35 (C=O), 148.28, 138.87, 132.90, 129.12, 127.72, 127.53, 123.92, 120.96, 120.15, 110.11 (ten aromatic carbons), 61.15, 58.99, 55.72, 48.52, 47.38, 30.74, 27.57, 25.29, 24.96 (nine aliphatic carbons); ESI-HRMS (*m/z*): found 457.1881 (M+H), calcd. 457.1881.

***N*-(2-Chlorophenyl)-1-((phenylsulfonyl)prolyl)pyrrolidine-2-carboxamide (8f):** White solid, yield: 0.96 g, 73%, m.p.: 158-159 ºC, FTIR (KBr, ν_{max}, cm^{-1}): 3314, 3276 (NH), 3193, 3115, 3062 (C-H arom.), 2930, 2854 (C-H aliph.), 1696, 1643 (2×C=O), 1591, 1537, 1490, 1447 (C=C arom.), 1393, 1348 (2×S=O), 1290, 1248, 1160, 1117 (S-N), 1096, 1072, 1022, 1007 (C-N); ^{1}H NMR (400 MHz, chloroform-d_6, δ ppm): 9.52 (s, 1H), 7.90-7.83 (m, 2H), 7.55 (dt, *J* = 33.1, 7.4 Hz, 3H), 7.39 (d, *J* = 8.8 Hz, 2H), 7.25 (d, *J* = 4.5 Hz, 2H), 4.69 (dd, *J* = 7.1, 3.5 Hz, 1H), 4.46-4.39 (m, 1H), 3.75 (t, *J* = 6.4 Hz, 2H), 3.55-3.44 (m, 1H), 3.37-3.26 (m, 1H), 2.25 (dd, *J* = 9.4, 5.6 Hz, 1H), 2.07 (dtt, *J* = 24.3, 12.6, 6.4 Hz, 5H), 2.00-1.94 (m, 1H), 1.83 (s, 1H); ^{13}C NMR (400 MHz, chloroform-d_6, δ ppm): 171.33 (C=O), 169.61 (C=O), 137.53, 137.34, 132.88, 131.30, 129.03, 127.19, 121.02, 116.01 (eight aromatic carbons), 61.47, 60.23, 48.46, 47.41, 30.19, 27.75, 25.17, 24.59 (eight aliphatic carbons); ESI-HRMS (*m/z*): found 461.1367 (M+H), calcd. 461.1367.

***N*-(4-Fluorophenyl)-1-((phenylsulfonyl)prolyl)pyrrolidine-2-carboxamide (8g):** Shiny black solid, yield: 2.8 g, 88%, m.p.: 155-156 ºC, FTIR (KBr, ν_{max}, cm^{-1}): 3374 (NH), 2926 (C-H arom.), 2854 (C-H aliph.), 1673 (C=O), 1599, 1530, 1488, 1461, 1436, 1405 (C=C arom.), 1345, 1305 (2×S=O), 1189, 1116 (S-N), 1092, 1047, 1027, 998 (C-N, C-O); ^{1}H NMR (400 MHz, chloroform-d_6, δ ppm): 8.32-8.23 (m, 2H), 7.72 (d, *J* = 8.2 Hz, 2H), 7.64 (t, *J* = 5.8 Hz, 1H), 7.33 (d, *J* = 8.1 Hz, 2H), 7.02 (t, *J* = 8.5 Hz, 1H), 6.96-6.80 (m, 2H), 4.26-4.02 (m, 3H), 3.83 (s, 3H), 3.60 (t, *J* = 7.0 Hz, 1H), 3.19 (dd, *J* = 9.8, 6.6 Hz, 1H), 2.42 (s, 3H), 2.13 (s, 1H), 1.89 (s, 1H), 1.79 (d, *J* = 7.9 Hz, 1H), 1.23 (s, 1H). ^{13}C NMR (400 MHz, chloroform-d_6, δ ppm): 172.03 (C=O), 166.42 (C=O), 148.08, 144.34, 132.30, 129.83, 127.67, 126.77, 123.96, 120.68, 120.11, 109.86 (ten aromatic carbons), 62.31, 55.42, 49.70, 43.97, 30.21, 24.17, 21.38 (seven aliphatic carbons); ESI-HRMS (*m/z*): found 445.1202 (M+H), calcd. 445.1201.

***N*-Phenyl-1-((phenylsulfonyl)prolyl)pyrrolidine-2-carboxamide (8h):** White solid, yield: 1.50 g, 56%, m.p.: 132-133 ºC; FTIR (KBr, ν_{max}, cm^{-1}): 3355 (NH), 3034, (C-H aromatic), 2925 2873 (C-H aliph.), 1667 (C=O), 1598, 1515, 1450, 1404 (C=C arom.), 1340, 1248 (2×S=O), 1191, 1158, 1121 (S-N), 1092, 1057, 1030 (C-N); ^{1}H NMR (400 MHz, chloroform-d_6, δ ppm): 8.62 (s, 1H), 7.73 (t, *J* = 8.1 Hz, 2H), 7.51 (d, *J* = 8.4 Hz, 2H), 7.35 (d, *J* = 8.1 Hz, 2H), 7.04 (d, *J* = 8.3 Hz, 2H), 4.47 (dd, *J* = 17.1, 8.1 Hz, 1H), 3.99 (dd, *J* = 9.0, 4.4 Hz, 1H), 3.82 (dd, *J* = 17.1, 4.7 Hz, 1H), 3.66-3.56 (m, 1H), 3.19-3.08 (m, 1H), 2.81 (s, 1H), 2.43 (s, 3H), 2.25 (s, 3H), 2.00 (dd, *J* = 9.5, 5.4 Hz, 2H), 1.59-1.51 (m, 1H), 1.23 (s, 1H); ^{13}C NMR (400 MHz, chloroform-d_6, δ ppm): 171.84 (C=O), 166.95 (C=O), 144.68, 135.06, 133.53, 131.33, 129.94, 129.04, 127.78, 119.85 (eight aromatic carbons), 62.33, 49.87, 43.44, 30.79, 24.26, 21.40, 20.65 (seven aliphatic carbons); ESI-HRMS (*m/z*): found 427.5200 (M+H), calcd. 427.5200.

Antioxidant activity

DPPH assay: The radical scavenging activity of the compounds was evaluated by DPPH assay as reported [34].

$$\text{DPPH radical scavenging activity (\%)} = \frac{A_{control} - A_{sample}}{A_{control}} \times 100$$

The half maximal concentration (IC_{50}) values were determined from the percentage inhibition using linear regression.

***In vivo* evaluation of anti-inflammatory activity:** The *in vivo* anti-inflammatory activity was carried out according to literature method [34]. In brief, male albino rats (average weight of approximately 280 ± 20 g) were obtained from the Animal House of the Department of Biochemistry, Nnamdi Azikiwe University, Awka, Nigeria. The animals were housed under controlled light and temperature conditions and were allowed free access to water but fasted for 15 h prior to the experiment. Ethical approval for animal use was obtained from the University Animal Ethics Committee (Approval No.: PG/Ph.D./16/80364).

Indomethacin (10 mg/kg) served as the standard reference drug, while the test compounds were suspended in 0.5% methylcellulose. The animals were divided into groups of five rats each: negative control (vehicle only), positive control (indomethacin) and test compound groups. Treatments were administered orally 1 h before induction of inflammation.

Acute inflammation was induced by sub-plantar injection of 0.3 mL of 1% carrageenan solution into the left hind paw. Paw volume was measured using a plethysmometer (Ugo Basile, Italy) immediately before and at 0.5, 1, 1.5, 2, 2.5 and 3 h after carrageenan injection. The percentage inhibition of paw edema was calculated using the following formula:

$$\frac{V_c - V_t}{V_c} \times 100$$

where V_c is the mean paw volume increase in control group; V_t is the mean paw volume increase in the treated group.

Data are expressed as percentage inhibition at each time. The anti-inflammatory activity was quantified by calculating the area under the inhibition–time curve (AUC) from 0.5 to 3 h using the trapezoidal rule. Statistical analysis was performed using one-way analysis of variance (ANOVA), followed by an appropriate post hoc multiple-comparison test to compare each test compound with the reference drug indomethacin. Differences were considered statistically significant at $p < 0.05$.

Antidiabetic activity: The antidiabetic potential of the synthesised dipeptide derivatives (**8a-h**) was evaluated using the alloxan-induced diabetes model in Wistar rats. Since diabetes mellitus is a metabolic disorder characterised by impaired carbohydrate and lipid metabolism, blood glucose, triglyceride and cholesterol levels were measured to assess the therapeutic efficacy of the test compounds.

Induction of experimental diabetes: Healthy male albino Wistar rats were acclimatised under standard laboratory conditions and subjected to an 18 h fast with free access to water prior to induction. Experimental diabetes was induced by a single intraperitoneal injection of alloxan monohydrate (120 mg/kg body weight) dissolved in physiological saline. To prevent the development of severe hypoglycemia during the early post-induction phase, the rats were provided with 5% dextrose solution *ad libitum* for 24 h after the alloxan administration. After 72 h, the development of hyperglycemia was confirmed by measuring fasting blood glucose using the tail tipping technique. Animals with fasting blood glucose levels above 200 mg/dL were considered diabetic and selected for further study. Baseline (day 0) values of glucose, triglycerides and cholesterol were recorded prior to treatment initiation [34].

Experimental design and treatment protocol: The animals were divided into 13 groups, each containing six rats, as follows: **Group 1**: Normal control (non-diabetic rats receiving vehicle only); **Group 2**: Diabetic control (alloxan-induced, untreated); **Group 3**: Diabetic rats treated with pioglitazone hydrochloride (10 mg/kg body weight, p.o.) for 12 consecutive days (standard drug control); **Groups 4-11**: Diabetic rats treated with synthesised dipeptide derivatives **8a-h** (100 mg/kg body weight, p.o.) once daily for 12 consecutive days.

Blood samples were collected from the tail vein at the intervals of 0, 3, 6, 9 and 12-days post-treatment for glucose estimation. Furthermore, triglyceride and total cholesterol levels were determined on days 0, 6 and 12 to evaluate the effects of compounds on lipid metabolism. All experimental procedures involving animals were reviewed and approved by the Institutional Animal Ethics Committee of the Department of Biochemistry, Nnamdi Azikiwe University, Awka, Nigeria in accordance with internationally accepted guidelines for the care and use of laboratory animals.

***In silico* pharmacokinetics and toxicity properties (ADMET):** The pharmacokinetics, brain or intestine permeation (BOILED-Egg) properties of the compounds were evaluated *in silico* using SwissADME tool based on the methodology. The computed descriptors include molecular weight, hydrogen bond donor and acceptor, number of rotatable bonds, topological polar surface area, logarithm of the partition coefficient, as well as their inhibition properties with CYP1A2, CYP2C9, CYP2D6 and CYP3A4. The toxicological profile of the compounds was evaluated using Pro-Tox II. The structures of the synthesised compounds were drawn using ChemDraw Professional 22.2.0.3300 and their simplified molecular input line entry system (SMILES) was generated and submitted to SwissADME or Pro-Tox-II tool for computation [35].

***In silico* drug-likeness:** The molecular properties that affect the bioavailability of drug candidates according to Lipinski's and Verber's rules were computed using SwissADME free online tool (http://www.swissadme.ch/). According to Lipinski's rule, compounds are more likely to be drug-like and orally bioavailable, if they do not fail in more than two of the following criteria: molecular weight ≤ 500, hydrogen bond donor ≤ 5, hydrogen bond acceptor ≤ 10, octanol/water partition coefficient ≤ 5 and rotatable bond count ≤ 10.

***In silico* molecular docking:** Molecular docking studies were carried out against selected protein targets such as human peroxiredoxin 5 (PDB: 1HD2), phosphodiesterase 4 (PDB: 4WCU) and peroxisome proliferator-activated receptor (PPAR) (PDB: 5u46) obtained from RCSB protein data bank. Molecular docking was carried out according to reported procedure using Autodock Vina PyRx, whereas ligand-protein interaction was visualised and analysed using BIOVIA Discovery Studio Visualizer client 21.1.0.20298 [36]. The structures of the synthesised compounds were drawn using ChemDraw and were assigned proper 3D orientation in Discovery Studio and then used as input for AutoDock Vina for docking simulation. The crystal structure of the select targets was downloaded from RCSB protein data bank and were prepared for docking using standard protocol, which includes deletion of side chains, heteroatoms and water of crystallisation, followed by energy minimisation and addition of polar hydrogen. Re-docking technique was used to validate the correctness of ligand-protein docking protocol. The co-crystallised ligand was initially withdrawn from the active site and re-docked into the prepared protein file. The grid box containing the binding site parameters was set to accommodate the region of interest using the graphical user interface program. AutoDock Vina was set to 8 exhaustiveness and non-specific algorithm was used to generate ligand-protein docked poses. The conformation with the lowest binding energy was further analysed to obtain the ligand-protein interactions using Discovery Studio [36].

RESULTS AND DISCUSSION

The synthesis of the pro-pro dipeptide-sulfonamides started with the sulfonamidation of *L*-proline with toluenesulfonyl chloride to form compound **2** in quantitative yield. The NH group of *L*-proline was protected with Boc to deliver compound **4**, which reacted with substituted amines **5a-h** in the presence of 1-ethyl-3-(3-dimethylaminopropyl)carbodiimide hydrochloride (EDC·HCl) coupling agent and 1-hydroxybenzotriazole (HOBt) as an additive to give amines **6a-h**. Trifluoroacetic acid in DCM was employed to cleave the Boc group in compounds **6a-h** to obtain compounds **7a-h**. Then, subsequent reaction of **7a-h** with compound **3** mediated by EDC·HCl and HOBt produced the target dipeptide-sulfonamides **8a-h** in good to excellent yields. The structural characterisation of the synthesised compounds was accomplished using spectroscopic methods.

The spectral and analytical data of synthesized dipeptide compounds **8a-h** confirm the successful synthesis of the sulphonamide-linked pro-pro dipeptide derivatives. The FTIR spectra display characteristic bands corresponding to the major functional groups in the molecular framework. Broad absorptions in the region 3407-3314 cm^{-1} are assigned to N–H stretching vibrations of amide groups, while aromatic and aliphatic C–H

stretching bands appear within 3193-3034 cm^{-1} and 2952-2854 cm^{-1}, respectively. Strong bands observed around 1696-1643 cm^{-1} correspond to amide carbonyl stretching vibrations, confirming formation of the dipeptide backbone. The sulphonamide functionality is supported by characteristic S=O stretching bands in the 1393-1305 cm^{-1} region and S–N vibrations near 1191-1115 cm^{-1}.

The ^{1}H NMR spectra are consistent with the proposed structures. A downfield singlet at δ 8.3-9.5 ppm is attributed to the amide NH proton, confirming peptide bond formation. The aromatic protons resonate within δ 6.8-7.9 ppm, whereas signals between δ 4.8-3.2 ppm correspond to methine and methylene protons adjacent to nitrogen atoms in the pyrrolidine and peptide framework. Aliphatic protons of the proline rings appear in the δ 2.5-1.2 ppm region. Methoxy-substituted derivatives show characteristic OCH_3 singlets near δ 3.8 ppm. The ^{13}C NMR spectra further support the assigned structures, with amide carbonyl carbons appearing in the δ 166-172 ppm range. Aromatic carbons resonate between δ 110-149 ppm, while carbons attached to nitrogen atoms appear in the δ 60-45 ppm region and the aliphatic carbons of the proline moieties are observed between δ 30-18 ppm. The ESI-HRMS spectra exhibit molecular ion peaks [$(M+H)^+$] that closely match the calculated *m/z* values for all compounds, confirming their molecular compositions and purity.

Antioxidant activity: The antioxidant potential of the synthesised dipeptide derivatives (**8a-h**) was assessed using DPPH radical scavenging assay (Table-1). All compounds showed varying degrees of radical scavenging activity, with IC_{50} values ranging from 0.214 μg/mL to 1.310 μg/mL. Compound **8g** exhibited the strongest antioxidant activity (IC_{50} = 0.214 μg/mL), comparable to ascorbic acid (0.213 μg/mL). Other potent derivatives included **8e** (0.344 μg/mL), **8d** (0.420 μg/mL) and **8h** (0.433 μg/mL).

Antioxidant activity and structure–activity correlation: The strong antioxidant activity of compound **8g** can be attributed to the electronic influence of the fluorine substituent. Due to its strong electronegativity, fluorine exerts a significant inductive electron-withdrawing effect that contributes to stabilization of radical intermediates, while also allowing partial delocalisation of unpaired electron density within the molecular framework. Ni & Hu [37] reported that α-fluorination markedly influences radical geometry and stability, where mono- and difluorinated systems exhibit enhanced radical persistence through a balance of inductive withdrawal and resonance stabilisation, whereas trifluorinated analogues display reduced stability due to limited resonance contribution.

Furthermore, fluorinated sulfonyl systems were shown to possess lower reduction potentials, facilitating single-electron transfer (SET) processes and improving radical generation and stabilisation. These electronic effects provide a plausible mechanistic explanation for the enhanced antioxidant activity observed for compound **8g**, highlighting the role of fluorine substitution in promoting favourable redox behaviour and radical stabilisation [37]. Compounds **8e** (4-Me), **8d** (H) and **8h** (2,4-Cl) also exhibited potent antioxidant activity (IC_{50} = 0.344-0.433 μg/mL), which can be rationalised by the optimal balance between hydrophobicity and electron-donating potential that favours radical neutralisation. Kancheva [38] demonstrated that monophenolic antioxidants containing electron donating substituents at the *ortho*-position exhibit enhanced radical-scavenging activity due to efficient electron donation. In addition, QSAR analysis revealed that antioxidant potency is strongly influenced by the hydrophilic–lipophilic balance of molecules, where increased lipophilicity promotes radical stabilisation and chain-breaking efficiency. These factors provide a plausible explanation for the strong antioxidant activity observed for compounds **8e**, **8d** and **8h**. In contrast, compounds **8a** and **8f** showed comparatively lower antioxidant activity, likely due to steric hindrance caused by bulky substituents. Kancheva [38] further reported that excessive steric bulk around the aromatic framework can hinder hydrogen atom transfer and electron donation processes, thereby reducing radical-scavenging efficiency. These observations explain the comparatively weaker antioxidant behaviour of compounds **8a** and **8f**.

***In vivo* anti-inflammatory activity:** According to the observed results (Table-2), all compounds exhibited significant ($p < 0.05$) inhibitory activity at 0.5 h post administration, with percentage inhibition ranging from 86.64-97.67%, surpassing that of indomethacin (71.55%). Among them, compounds **8c** and **8h** demonstrated the most potent early-phase activity (97.67% and 97.56%, respectively). Percentage inhibition of inflammation progressively decreased for all treated groups from 1 h post administration, slightly different from the indomethacin treated group which peaked at 1 h post administration

TABLE-1
DPPH RADICAL SCAVENGING ACTIVITY DATA OF SYNTHESISED DIPEPTIDE DERIVATIVES (8a-h) (MEAN ± SEM, n = 3)

Concentration (μg/mL)	Radical inhibition of the compounds (%)			
	200	100	50	IC_{50}
8a	50.80 ± 0.003	70.35 ± 0.003	53.60 ± 0.002	1.221
8b	64.60 ± 0.002	75.25 ± 0.001	80.60 ± 0.003	0.870
8c	55.46 ± 0.003	61.49 ± 0.002	72.60 ± 0.001	1.242
8d	80.80 ± 0.001	87.42 ± 0.001	75.60 ± 0.001	0.420
8e	86.83 ± 0.003	79.27 ± 0.003	80.60 ± 0.002	0.344
8f	61.80 ± 0.004	54.96 ± 0.003	47.60 ± 0.002	1.310
8g	94.85 ± 0.003	89.96 ± 0.003	87.60 ± 0.003	0.214
8h	82.67 ± 0.001	79.42 ± 0.003	81.60 ± 0.002	0.433
Ascorbic acid	96.88 ± 0.001	91.80 ± 0.003	87.60 ± 0.002	0.213

Data are means ± standard deviations of triplicate experiments

TABLE-2
TIME-DEPENDENT PERCENTAGE INHIBITION AND AREA UNDER THE INHIBITION-TIME CURVE (AUC) OF SYNTHESISED COMPOUNDS **8a-h** AND INDOMETHACIN AT FIXED DOSE

Compound	0.5 h	1 h	1.5 h	2 h	2.5 h	3 h	AUC (0.5–3 h)
8a	86.64	85.83	81.27	80.42	77.12	70.07	201.50
8b	95.10	94.13	87.75	80.67	79.94	77.34	214.36
8c	97.67	91.89	82.94	82.48	78.34	78.07	211.76
8d	93.74	83.89	81.51	79.34	76.22	73.77	202.36
8e	88.56	84.75	83.84	78.98	78.34	72.45	203.21
8f	95.78	92.88	90.44	80.42	79.25	76.56	214.58
8g	90.34	84.58	81.36	80.67	70.44	69.34	198.45
8h	97.56	90.24	86.23	83.67	83.00	78.07	215.48
Indomethacin	71.55	78.66	76.57	71.00	68.67	66.64	182.00

Data are presented as percentage inhibition at the indicated time points. Inset shows area under the inhibition–time curve (AUC, 0.5-3 h). Statistical significance *versus* indomethacin was assessed by one-way ANOVA followed by post hoc analysis ($p < 0.05$).

(78.66%), then decreased progressively throughout the duration of the experiment.

During the later phase (2-3 h), compound **8h** maintained the highest inhibition at 2 h (83.67%), 2.5 h (83.00%) and 3 h (78.07%) alongside compound **8c** (78.07%). Percentage inhibition for all treatment groups remained consistently higher than the indomethacin treated group throughout the observation period and the overall potency trend was **8h** ≈ **8c** > **8b** > **8f** > **8d** > **8e** > **8a** > **8g** > indomethacin.

Anti-inflammatory activity and biphasic inflammation model: The carrageenan-induced rat paw edema model remains a gold standard for evaluating the anti-inflammatory potential of novel compounds because it reflects the biphasic nature of acute inflammation mediated first by histamine and serotonin release (0-1 h) and later by prostaglandins and other eicosanoids (1-3 h) [39,40]. In this study, all synthesised dipeptide derivatives (**8a-h**) demonstrated marked inhibition of paw edema, confirming their capacity to attenuate both early and late inflammatory processes.

At the early phase (0.5-1 h), test compounds exhibited superior inhibitory effects exceeding the activity of the reference drug indomethacin. This strong and rapid onset suggests that these compounds possess structural features capable of stabilizing mast cell membranes or antagonizing histamine and serotonin release at the site of inflammation. The high polarity and hydrogen-bonding potential of their peptide backbones likely contributed to this rapid tissue penetration and mediator interference [40].

During the late phase (1.5-3 h), compounds **8f**, **8c** and **8h** maintained significantly higher inhibition than indomethacin, suggesting downregulation of prostaglandin biosynthesis or inhibition of cyclooxygenase (COX) enzymes. This observation aligns with our earlier *in silico* predictions that the dipeptide scaffolds could bind favourably to the COX-2 active site *via* hydrogen bonding to key residues such as Tyr385 and Ser530 [41]. The sustained inhibition seen with compound **8h** (83.67% at 2 h and 83.00% at 2.5 h) implies a long-lasting anti-inflammatory effect that could be attributed to enhanced lipophilicity or aromatic substitution, which increases its interaction with hydrophobic pockets of the enzyme and prolongs biological activity [42].

Structure-activity relationships in anti-inflammatory activity: Structurally, subtle variations in side chain composition among the dipeptides appear to influence their pharmacological behaviour significantly. Compounds containing aromatic substituents (*e.g.* phenylalanine, tyrosine-derived fragments) or electron-withdrawing groups (such as halogens or carbonyl-rich side chains) exhibited stronger activity. These moieties likely enhance π-π stacking and hydrophobic interactions within enzyme binding sites, contributing to superior potency of compounds **8c** and **8h** [43].

The balance between hydrophilicity and lipophilicity proved crucial for bioavailability. Dipeptides that maintained moderate lipophilic character likely penetrated cell membranes more efficiently while retaining sufficient aqueous solubility for systemic distribution [44]. Compounds **8c** and **8h** appear to strike this optimal balance, explaining their superior and sustained anti-inflammatory activity.

The peptide bond itself confers flexibility and hydrogen-bonding potential, enabling multiple modes of interaction with biological targets. The amide linkages and terminal functional groups in active dipeptides could interact with catalytic residues or influence conformational stability of enzymes such as COX or lipoxygenase (LOX) [45]. Moreover, their potential antioxidant capacity, arising from phenolic or amide functionalities, may have indirectly contributed to inflammation reduction by scavenging reactive oxygen species that amplify inflammatory cascades [46].

Multimodal mechanism compared to indomethacin: When compared with indomethacin, which is a pure COX inhibitor acting primarily in the late prostaglandin-mediated phase, the dipeptides showed dual-phase inhibition, indicating a multimodal mechanism [47]. This could involve initial membrane stabilisation or cytokine suppression (early phase) and subsequent interference with arachidonic acid metabolism (late phase). Such dual mechanism enhances therapeutic value by providing both rapid and sustained anti-inflammatory responses with possibly reduced gastrointestinal side effects, which are typical of non-selective NSAIDs [48].

In vivo antidiabetic

Effect on blood glucose levels: Administration of all dipeptide derivatives to alloxan-induced diabetic rats resulted in a progressive and significant ($p < 0.05$) reduction in blood glucose levels compared with the diabetic control (Table-3). The highest reduction in blood glucose level in the dipeptide

TABLE-3
EFFECT OF SYNTHESISED COMPOUND ON BLOOD GLUCOSE LEVEL (mg/dL) IN ALLOXAN-INDUCED DIABETIC RATS (MEAN ± SEM, n = 6)

Group	0 day	3 day	6 day	9 day	12 day
Normal control	105.6 ± 7.1	106.4 ± 2.2	105.6 ± 2.6	106.5 ± 4.4	106.8 ± 7.5
Diabetic control	388.1 ± 1.3	360.2 ± 1.6	360.8 ± 1.3	361.2 ± 1.6	360.8 ± 4.6
Acarbose	382.3 ± 1.6	223.8 ± 1.7	148.3 ± 7.1	120.5 ± 8.1	106.5 ± 5.3
8a	372.1 ± 3.2	224.5 ± 3.3	140.2 ± 1.7	122.8 ± 7.2	105.4 ± 2.2
8b	391.7 ± 4.3	227.9 ± 4.2	155.8 ± 5.5	126.7 ± 8.1	118.3 ± 6.4
8c	356.3 ± 2.2	280.6 ± 3.3	206.3 ± 3.7	177.3 ± 2.4	134.5 ± 8.3
8d	387.4 ± 4.5	227.8 ± 1.7	162.6 ± 5.7	118.9 ± 3.0	111.5 ± 4.2
8e	381.7 ± 6.6	283.6 ± 5.7	159.3 ± 4.2	123.8 ± 8.6	112.7 ± 3.8
8f	371.8 ± 7.9	275.2 ± 5.5	169.2 ± 3.7	133.6 ± 5.4	125.2 ± 3.5
8g	362.7 ± 2.6	264.6 ± 3.6	181.6 ± 6.6	145.8 ± 6.2	117.3 ± 5.7
8h	365.3 ± 6.8	271.4 ± 3.7	177.8 ± 2.9	139.4 ± 2.9	120.5 ± 4.3

Data are means ± standard deviations of triplicate experiments.

administered groups was observed with compound **8a** (105.4 ± 2.2 mg/dL at day 12), comparable to acarbose (106.5 ± 5.3 mg/dL on the same day). Compounds **8d** and **8e** also exhibited marked hypoglycemic effects by Day-12 following treatments. The test compounds showed a time-dependent hypoglycemic effect in diabetic rats, with progressive improvement across the 12-day treatment period.

Effect on blood cholesterol levels: Treatment with dipeptide derivatives significantly reduced elevated serum cholesterol levels in diabetic rats (Table-4). After 6 days of administration, compounds **8d** (178.4 ± 2.4 mg/dL) and **8c** (181.6 ± 4.9 mg/dL), showed better cholesterol-lowering activity than acarbose (191.7 ± 5.4 mg/dL). The hypolipidemic effect was sustained through day 12 for all treated groups (133.4 ± 5.3 mg/dL–153.6 ± 3.8 mg/dL) and were within comparable levels to both the normal control (144.7 ± 5.4 mg/dL) and the acarbose treated group (131.4 ± 7.3 mg/dL).

TABLE-4
EFFECT OF SYNTHESISED COMPOUND ON TOTAL CHOLESTEROL LEVEL (mg/dL) IN ALLOXAN-INDUCED DIABETIC RATS (MEAN ± SEM, n = 6)

Group	0 day	6 day	12 day
Normal control	144.4 ± 3.5	140.4 ± 6.4	144.7 ± 5.4
Diabetic control	345.6 ± 4.7	347.6 ± 5.9	345.7 ± 7.7
Acarbose	336.8 ± 8.2	191.7 ± 5.4	131.4 ± 7.3
8a	357.3 ± 2.8	221.2 ± 1.4	133.4 ± 5.3
8b	349.4 ± 8.7	231.7 ± 6.4	141.5 ± 2.5
8b	367.6 ± 4.4	201.9 ± 2.7	133.4 ± 2.2
8c	355.8 ± 8.7	181.6 ± 4.9	152.6 ± 3.8
8d	367.3 ± 2.8	178.4 ± 2.4	143.3 ± 9.2
8e	359.4 ± 8.7	196.5 ± 3.2	134.4 ± 5.3
8f	367.6 ± 4.4	214.4 ± 1.8	153.6 ± 3.8
8h	356.3 ± 2.8	227.2 ± 1.4	144.3 ± 9.2

Data are means ± standard deviations of triplicate experiments.

Effect on blood triglyceride levels: All dipeptide derivatives demonstrated significant triglyceride-lowering activity relative to the diabetic control (Table-5). Compounds **8a**, **8b**, **8e** and **8f** produced the most notable reductions by day 12 (116.6 ± 2.3, 122.7 ± 8.5, 122.7 ± 8.5 and 120.6 ± 5.9 mg/dL, respectively), comparable to acarbose (115.6 ± 2.3 mg/dL) and normal control (122.5 ± 6.7 mg/dL).

TABLE-5
EFFECT OF NOVEL DIPEPTIDE DERIVATIVES (**8a-h**) ON TRIGLYCERIDE LEVEL (mg/dL) IN ALLOXAN-INDUCED DIABETIC RATS (MEAN ± SEM, n = 6)

Group	0 day	6 day	12 day
Normal control	122.5 ± 9.5	123.5 ± 8.5	122.5 ± 6.7
Diabetic control	252.6 ± 2.3	253.6 ± 3.4	252.6 ± 8.8
Acarbose	248.4 ± 5.2	186.5 ± 9.3	115.6 ± 2.3
8a	251.5 ± 7.9	218.8 ± 8.7	116.6 ± 2.3
8b	246.3 ± 6.3	223.9 ± 6.2	122.7 ± 8.5
8c	255.5 ± 5.5	222.6 ± 2.4	120.6 ± 5.9
8d	248.0 ± 2.8	222.6 ± 2.4	129.4 ± 4.5
8e	254.5 ± 7.9	203.8 ± 9.8	122.7 ± 8.5
8f	247.3 ± 6.3	218.6 ± 6.4	120.6 ± 5.9
8g	258.5 ± 5.5	212.9 ± 7.8	129.4 ± 4.5
8h	259.5 ± 5.5	224.6 ± 2.4	123.7 ± 8.5

Data are means ± standard deviations of triplicate experiments.

Antidiabetic activity and structure–activity relationship: All dipeptide derivatives significantly reduced blood glucose levels in alloxan-induced diabetic rats relative to untreated diabetic controls, with hypoglycemic effects becoming more pronounced with increasing treatment duration. Compound **8a** (R = 4-OMe) produced the highest hypoglycemic effect, achieving near-normal glycemic levels (105.4 ± 2.2 mg/dL) after 12 days, comparable to acarbose (106.5 ± 5.3 mg/dL). This enhanced activity can be attributed to the *para*-methoxy (–OCH_3) substituent, an electron-donating group that increases electron density on the aromatic ring, thereby enhancing hydrogen-bonding potential and interaction with active-site residues of carbohydrate-hydrolyzing enzymes such as α-glucosidase or α-amylase [49]. Halogen-substituted analogues (**8b**, **8f**, **8g**, **8h**) showed slightly lower glucose-lowering effects, consistent with the electron-withdrawing nature of halogens that can reduce electron density on amide nitrogen [50]. Nevertheless, their activity remained substantial, suggesting that halogen atoms contribute to hydrophobic or halogen-bond interactions with enzyme residues, stabilizing the ligand–protein complex. The relatively moderate activity of compounds **8c** (2,5-dimethyl) and **8e** (4-methyl) indicates that bulky hydrophobic groups might reduce binding affinity due to steric hindrance at the catalytic pocket. Compound **8d** (R = H) retained appreciable activity, indicating that the

unsubstituted phenyl ring provides a favourable scaffold but that substitution with small electron-donating groups further enhances potency [51].

Antihyperlipidemic effects: The lipid-lowering effects likely result from improved glycemic control mediated by these dipeptides, as chronic hyperglycemia is tightly coupled with dyslipidemia through altered hepatic lipid metabolism. The varying responses among analogues further suggest that electronic and steric substituent effects modulate affinity toward key metabolic enzymes such as AMP-activated protein kinase (AMPK) or lipoprotein lipase (LPL) [52].

***In silico* drug-likeness:** According to the results in Table-6, all the bioactive compounds showed good physio-chemical parameters. The molecular weight and the topological polar surface area of the compounds ranged from 427.52-506.41 g/mol and 95.17-104.40 Å^2 respectively. These parameters align with passive molecular transport through membranes, which suggest that the compounds have high membrane permeability. The number of rotatable bond carbon complied with Lipinski's and Verber's rule (*i.e.* ≤ 10), as higher values may lower bioavailability, membrane permeability, conformational entropy and binding affinity. Further, the lipophilicity index of the compounds, indicated by LogP remained ≤ 5, which ensures favourable oral bioavailability and membrane permeability. Other descriptors such as hydrogen bond donor and acceptor, which facilitate drug-receptor interactions for enhanced therapeutic action, remained within the ideal range. Moreover, all the compounds showed bioavailability score of 0.55, which indicate good physiochemical properties that support passive absorption and oral bioavailability. According to the bioavailability radar of the compounds depicted in Fig. 1, the optimum range of a particular property is indicated by

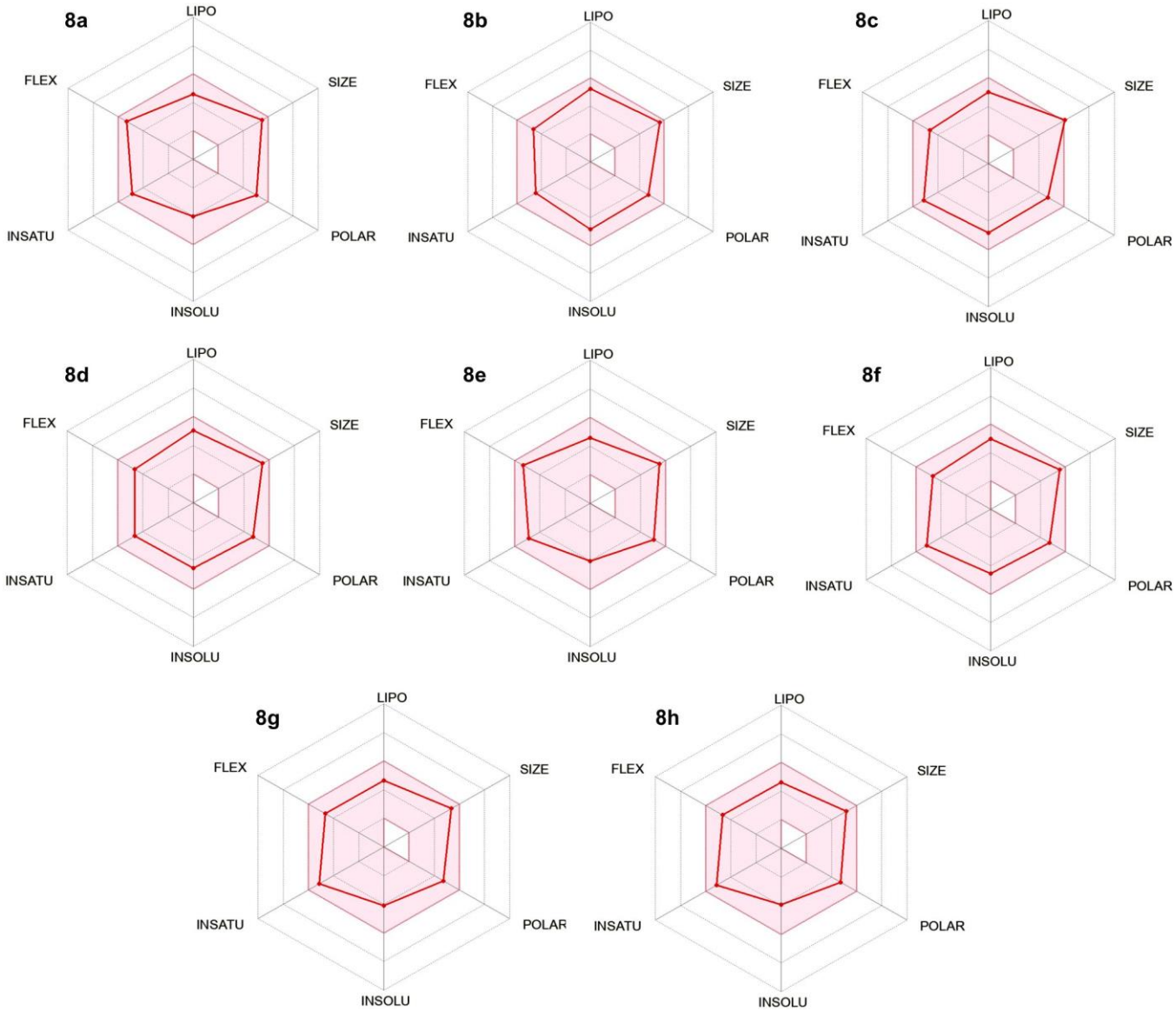

Fig. 1. Bioavailability radar of the synthesised compounds. The pink area indicates optimal range of particular descriptor; LIPO = lipophilicity as XLOGP3; SIZE = size as molecular weight; POLAR = polarity as TPSA (topological polar surface area); INSOLU = insolubility in water by log S scale; INSATU = insaturation as per fraction of carbons in the sp^3 hybridisation; FLEX = flexibility as per rotatable bonds

TABLE-6
PHYSICO-CHEMICAL PROPERTIES OF THE SYNTHESIZED COMPOUNDS

Compounds	MW	HBD	HBA	LogP	RBC	Lipinski's rule	TPSA (Å)	ABS	Csp^3
8a	457.54	1	6	2.01	8	0	104.40	0.55	0.39
8b	469.50	1	5	3.11	7	0	95.17	0.55	0.44
8c	506.41	1	5	2.66	7	1	95.17	0.55	0.36
8d	455.57	1	5	2.69	7	0	95.17	0.55	0.42
8e	457.55	1	6	2.07	8	0	104.40	0.55	0.39
8f	461..96	1	5	2.61	7	0	95.17	0.55	0.36
8g	445.51	1	6	2.36	7	0	95.17	0.55	0.36
8h	427.52	1	5	2.06	7	0	95.17	0.55	0.36
[a]	≤ 500	≤ 5	≤ 10	≤ 5	≤ 10	≤ 2	[b] ≤ 140	≥0.55	

MW: molecular weight of the molecule, HBD: number of hydrogen bonds that would be donated by the solute to water molecules in an aqueous solution, HBA: number of hydrogen bonds that would be accepted by the solute from water molecules in an aqueous solution, Rule of five: Number of violations of Lipinski's rule, Log P: water partition coefficient, RBC: approximated number of rotatable bonds, TPSA: topological polar surface area, ABS: a bioavailability score, Csp^3: the percentage of carbon atoms in a molecule that are sp^3 bonded.
[a]Recommended value based on Lipinski's rule; [b]Recommended value based on Verber's rule.

the pink region. Drug-likeness properties are defined by the red hexagon within the pink region. It follows that most of the compounds remained inside the optimal pink region.

The Egan BOILED-Egg predictive model was used to evaluate the passive absorption and brain penetration of the synthesised compounds and the results are presented in Table-7. Fig. 2 shows that all the compounds demonstrated no blood–brain barrier (BBB) permeability and exert high human gastrointestinal absorption (HIA) in the white region. The aqueous solubility of the compounds ranged from soluble to moderately soluble, as indicated by Log S (ESOL). Present studies showed that all the compounds are non-inhibitors of P_{450} 1A2 (CYP1A2), which play an important role in drug metabolism [34]. The toxicity of the compounds was evaluated using ProTox II server and the results indicated that the compounds belong to category IV with LD_{50} 1000 mg/kg. The low toxicity of the synthesised dipeptides derivatives further indicates their potential as drug candidates.

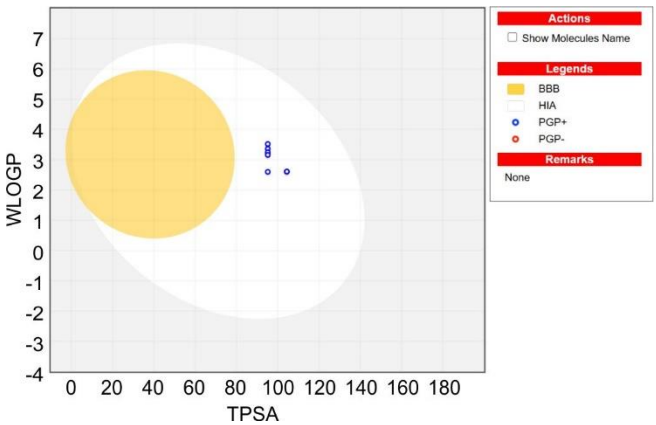

Fig. 2. Predicted BOILED-Egg diagram of the synthesised compounds

Conclusion

The structure–activity relationship (SAR) trends derived from this study indicate that substitution at the *para*-position with either electron-donating or halogen groups significantly influences the pharmacological profile of the synthesised dipeptide derivatives (**8a-h**). Compound **8a** (4-OMe) emerged as the most promising candidate, exhibiting superior antidiabetic and lipid-lowering activity, while **8g** (4-F) demonstrated the strongest antioxidant potential. Compounds **8c** and **8h** showed consistent and high anti-inflammatory inhibition across all time points, suggesting favourable pharmacodynamic and pharmacokinetic attributes. The findings indicated that aromatic substitution, moderate lipophilicity and hydrogen-bonding capacity are the key determinants of bioactivity across multiple therapeutic endpoints. The combined data suggest that these structural frameworks could serve as valuable templates for the development of multi-target anti-inflammatory and antidiabetic agents with concurrent antioxidant benefits. To further validate these observations, future mechanistic studies should include *in vitro* COX-1/COX-2 enzyme inhibition assays, molecular docking and molecular dynamics simulations to confirm binding affinity and selectivity, along with cytokine profiling to elucidate their effects on pro-inflammatory mediators.

TABLE-7
CALCULATED MOLECULAR PROPERTIES AND PHARMACOKINETICS PARAMETERS

Compound	Log S	BBB	GI	P-gp	Log Kp (cm/s)	CYP1A2
8a	MS	No	High	Yes	-7.30	No
8b	MS	No	High	Yes	-6.58	No
8c	MS	No	High	Yes	-7.09	No
8d	MS	No	High	Yes	-6.75	No
8e	MS	No	High	Yes	-7.30	No
8f	MS	No	High	Yes	-6.87	No
8g	MS	No	High	Yes	-7.14	No
8h	S	No	High	Yes	-7.10	No

CONFLICT OF INTEREST

The authors declare that there is no conflict of interests regarding the publication of this article.

DECLARATION OF AI-ASSISTED TECHNOLOGIES

During the preparation of this manuscript, the authors used an AI-assisted tool(s) to improve the language. The authors reviewed and edited the content and take full responsibility for the published work.

REFERENCES

1. M.E. de Oliveira, G. Cenzi, R.R. Nunes, C.R. Andrighetti, D.M. de S. Valadão, C. dos Reis, C.M.O. Simões, R.J. Nunes, M.C. Júnior, A.G. Taranto, B.A.M. Sanchez, G.H.R. Viana and F. de P. Varotti, *Molecules*, **18**, 15276 (2013); https://doi.org/10.3390/molecules181215276
2. A. L. Svogi, M. Isaacs, H. Hoppe, S. Khane and C. Veale, *Eur. J. Med. Chem.*, **114**, 79 (2016); https://doi.org/10.1016/j.ejmech.2016.02.056
3. B. Mistry, K. Desai and S. Intwala, *Indian J. Chem.*, **54B**, 128 (2015).
4. B. Nubia, C. Luiz, A. Osvaldo and C. Isabor, *Molecules*, **16**, 8083 (2011); https://doi.org/10.3390/molecules16098083
5. J. Dominguez, C. Leon, J. Rodrigues, N. de Dominguez, J. Gut and P.J. Rosenthal, *IL Farmaco*, **60**, 307 (2005); https://doi.org/10.1016/j.farmac.2005.01.005
6. K. Parai, G. Panda, K. Srivastava and S. Pur, *Bioorg. Med. Chem. Lett.*, **18**, 776 (2008); https://doi.org/10.1016/j.bmcl.2007.11.038
7. C. Montalbetti and V. Falque, *Tetrahedron*, **61**, 10827 (2005); https://doi.org/10.1016/j.tet.2005.08.031
8. D. Ugwu, B. Ezema, F. Eze and D. Ugwuja, *Int. J. Med. Chem.*, **2014**, 614808 (2014); https://doi.org/10.1155/2014/614808
9. M. Ghorab, M. Bashandy and M. Alsaid, *Acta Pharm.*, **64**, 419 (2014); https://doi.org/10.2478/acph-2014-0035
10. Ö. İdil, H. Şahal, E. Canpolat and M. Özkan, *Indones. J. Chem.*, **23**, 831 (2023); https://doi.org/10.22146/ijc.83873
11. D. Ugwu, U. Okoro and N. Mishra, *Eur. J. Med. Chem.*, **135**, 349 (2017); https://doi.org/10.1016/j.ejmech.2017.04.029
12. T. Day and S. Greenfield, *Exp. Brain Res.*, **155**, 500 (2004); https://doi.org/10.1007/s00221-003-1757-1
13. V.Kh. Khavinson and V. Anisimov, *Dokl. Akad. Nauk.*, **372**, 421 (2000).
14. P. Jatinder, S. Singh and N. Sethi, *Orient. J. Chem.*, **31**, 417 (2015); https://doi.org/10.13005/ojc/310149
15. H. Kayser and H. Meisel, *FEBS Lett.*, **383**, 18 (1996); https://doi.org/10.1016/0014-5793(96)00207-4
16. A. Thomson, W. Liu, E. Chun, V. Katritch, H. Wu and E. Vardy, *Nature*, **485**, 495 (2012); https://doi.org/10.2210/pdb4ea3/pdb
17. J. Ezugwu, U. Okoro, M. Ezeokonkwo, C. Bhimapaka, S. Okafor and D. Ugwu, *Arch. Pharm.*, **353**, 1 (2020); https://doi.org/10.1002/ardp.202000074
18. S. Panda, M. Kucukbay, H. Meyers, M. Sverdrup and F. El-Feky, *Chem. Biol. Drug Des.*, **82**, 361 (); https://doi.org/10.1111/cbdd.12134
19. A. Festa, R. D'Agostino, G. Howard, L. Mykkänen, R. Tracy and S. Haffner, *Circulation*, **102**, 42 (2000); https://doi.org/10.1161/01.CIR.102.1.42
20. M. Frohlich, A. Imhol and G. Berg, *Diabetes Care*, **23**, 1835 (2000); https://doi.org/10.2337/diacare.23.12.1835
21. M. Crook, *Diabet. Med.*, **21**, 203 (2004); https://doi.org/10.1046/j.1464-5491.2003.01030.x
22. F. Giacco and M. Brownlee, *Circ. Res.*, **107**, 1058 (2010); https://doi.org/10.1161/CIRCRESAHA.110.223545
23. A. K. Tewari, V. P. Singh, P. Yadav, G. Gupta, A. Singh, R. K. Goel, P. Shinde and C. G. Mohan, *Bioorg. Chem.*, **56**, 8 (2014); https://doi.org/10.1016/j.bioorg.2014.05.004
24. J. M. Scheiman, *Clin. Update*, **12**, 1 (2005); https://doi.org/10.1016/j.clinup.2004.10.001
25. International Diabetes Federation, IDF Diabetes Atlas, Brussels, Belgium, edn 10 (2021); http://www.diabetesatlas.org
26. R.P. Dash, R.J. Babu and N.R. Srinivas, *Xenobiotica*, **48**, 89 (2018); https://doi.org/10.1080/00498254.2016.1275063
27. H.M. Kim and C.G. Hyun, *Molecules*, **28**, 115 (2022); https://doi.org/10.3390/molecules28010115
28. P. Sharma, G.D. Gupta and V. Asati, *Bioorg. Chem.*, **139**, 106750 (2023); https://doi.org/10.1016/j.bioorg.2023.106750
29. F.C. Asogwa, U.D. Izuchukwu, H. Louis, C.C. Eze, C.M. Ekeleme, J.A. Ezugwu, I. Benjamin, S.I. Attah, E.C. Agwamba, O.C. Ekoh and A.S. Adeyinka, *Polycycl. Aromat. Compd.*, **43**, 8690 (2023); https://doi.org/10.1080/10406638.2022.2150653
30. I.O. Christian, O.U. Christopher, A.C. Chris, O.N. Marytheresa, U.D. Izuchukwu, N.R. Chinyere, O.K. John, O.N. Paul, O.N. Johnson, E.C. Chibuike and A.S. Izuchukwu, *Am. J. Appl. Sci. Res.*, **9**, 109 (2023).
31. S.I. Attah, U.C. Okoro, S.P. Singh, C.C. Eze, C.U. Ibeji, J.A. Ezugwu, O.U. Okenyeka, O. Ekoh, D.I. Ugwu and F.U. Eze, *J. Mol. Struct.*, **1264**, 133280 (2022); https://doi.org/10.1016/j.molstruc.2022.133280
32. J.A. Ezugwu, U.C. Okoro, M.A. Ezeokonkwo, C. Bhimapaka, S.N. Okafor and D.I. Ugwu, *Arch. Pharm.*, **353**, 2000074 (2020); https://doi.org/10.1002/ardp.202000074
33. J.A. Ezugwu, U.C. Okoro, M.A. Ezeokonkwo, K.S. Hariprasad, M. Rudrapal, N. Gogoi, D. Chetia, D.I. Ugwu, F.U. Eze, L.E. Onyeyilim and C.C. Eze, *Chem. Afr.*, **7**, 2353 (2024); https://doi.org/10.1007/s42250-024-00904-7
34. S.I. Attah, I.V. Okonkwo, U.C. Okoro, N. Orji, J.A. Ezugwu, D.I. Ugwu, C. Ibeji, A.E. Onoabedje, L.A. Ogara, P.S. Singh, F.N. Ibeanu and C.C. Eze, *Chem. Afr.*, **8**, 1889 (2025); https://doi.org/10.1007/s42250-025-01266-4
35. P. Banerjee, A.O. Eckert, A.K. Schrey and R. Preissner, *Nucleic Acids Res.*, **46**, W257 (2018); https://doi.org/10.1093/nar/gky318
36. BIOVIA Dassault Systèmes, BIOVIA Discovery Studio Visualizer, ver. 21.1.0.20298. San Diego, CA, USA (2021).
37. C. Ni and J. Hu, *Chem. Soc. Rev.*, **45**, 5441 (2016); https://doi.org/10.1039/C6CS00351F
38. V.D. Kancheva, *Eur. J. Lipid Sci. Technol.*, **111**, 1072 (2009); https://doi.org/10.1002/ejlt.200900005
39. I. Posadas, M. Bucci, F. Roviezzo, A. Rossi, L. Parente, L. Sautebin, and G. Cirino, *Br. J. Pharmacol.*, **142**, 331 (2004); https://doi.org/10.1038/sj.bjp.0705650
40. L.L. de Siqueira Patriota, D. de Brito Marques Ramos, M. Gama e Silva, A.C.L. Amorim dos Santos, Y. Araújo Silva, P.M.G. Paiva, E.V. Pontual, L.P. de Albuquerque, R.L. Mendes and T.H. Napoleão, *Polymers*, **14**, 1609 (2022); https://doi.org/10.3390/polym14081609
41. M. Miciaccia, B. D. Belviso, M. Iaselli, G. Cingolani, S. Ferorelli, M. Cappellari, P. Loguercio Polosa, M.G. Perrone, R. Caliandro and A. Scilimati, *Sci. Rep.*, **11**, 4312 (2021); https://doi.org/10.1038/s41598-021-83438-z
42. T. Constantinescu, C. N. Lungu and I. Lung, *Molecules*, **24**, 1505 (2019); https://doi.org/10.3390/molecules24081505
43. W. Liu, X. Chen, H. Li, J. Zhang, A. An and X. Liu, *Foods*, **11**, 2361 (2022); https://doi.org/10.3390/foods11152361
44. A. Visconti, G. Ermondi, G. Caron and R. Esposito, *J. Comput. Aided Mol. Des.*, **29**, 361 (2015); https://doi.org/10.1007/s10822-015-9829-4
45. J.C. Jiménez-Cruz, R. Guzmán-Mejía, P. Navarro-Santos, H.A. García-Gutiérrez, J.C. Ontiveros-Rodríguez, R. Herrera-Bucio and J. A. Aviña-Verduzco, *Chem. Proc.*, **16**, 95 (2023); https://doi.org/10.3390/ecsoc-28-20256
46. C. F. Manful, E. Fordjour, D. Subramaniam, A. A. Sey, L. Abbey and R. Thomas, *Int. J. Mol. Sci.*, **26**, 7520 (2025); https://doi.org/10.3390/ijms26157520
47. K. R. A. Abdellatif, P. F. Lamie and H. A. Omar, *J. Enzyme Inhib. Med. Chem.*, **31**, 318 (2016); https://doi.org/10.3109/14756366.2015.1022174
48. K. Abuelella, S. Mosallam, S. Soliman and A. Elshafeey, *Bull. Pharm. Sci. Assiut Univ.*, (2025); https://doi.org/10.21608/bfsa.2025.400585.2621
49. S. Dadashpour, *Med. Chem. Res.*, **34**, 945 (2025); https://doi.org/10.1007/s00044-025-03390-9
50. T.J. Lampidis, M. Kurtoglu, J.C. Maher, H. Liu, A. Krishan, V. Sheft, S. Szymanski, I. Fokt, W.R. Rudnicki, K. Ginalski, B. Lesyng and W. Priebe, *Cancer Chemother. Pharmacol.*, **58**, 725 (2006); https://doi.org/10.1007/s00280-006-0207-8
51. T.H.T. Phan, K. Hengphasatporn, Y. Shigeta, W. Xie, P. Maitarad, T. Rungrotmongkol and W. Chavasiri, *ACS Omega*, **8**, 26340 (2024); https://doi.org/10.1021/acsomega.3c02868
52. B.B. Kakoti, S. Alom, K. Deka and R.K. Halder, *J. Diabetes Metab. Disord.*, **23**, 441 (2024); https://doi.org/10.1007/s40200-024-01420-8